Design of a Ku-Band High-Purity Transducer for the TM_{01} Circular Waveguide Mode by Means of T-Type Junctions

JOSÉ R. MONTEJO-GARAI [1], JORGE A. RUIZ-CRUZ [2], (Senior Member, IEEE), AND JESÚS M. REBOLLAR[1], (Member, IEEE)

[1]Grupo de Electromagnetismo Aplicado, Information Processing and Telecommunications Center, Universidad Politécnica de Madrid, 28040 Madrid, Spain
[2]Escuela Politécnica Superior, Universidad Autónoma de Madrid, 28049 Madrid, Spain

Corresponding author: José R. Montejo-Garai (joseramon.montejo@upm.es)

ABSTRACT A new mode transducer for converting the TE_{10} rectangular waveguide mode to the TM_{01} circular waveguide mode is presented. The novel topology is based on two T-type junctions with in-phase excitation at their input rectangular ports. The first one is an H-plane T-junction in rectangular waveguide. The second one differs from the standard E-plane T-junction in the excitation, which is carried out by modes excited with fields having the same in-phase polarization at the input rectangular ports, and has the output port in circular waveguide. This configuration exploits the symmetry of the modes under consideration to achieve a high-purity conversion, controlling the propagating circular waveguide TE_{11} mode to a maximum level of -42 dB in the whole operation band. The design bandwidth is 2 GHz centered at 12 GHz with a return loss level higher than 28 dB. In addition, the transducer can be divided in a main body plus a cover for easing the manufacturing. In order to verify the proposed geometry, a back-to-back arrangement has been measured connecting two similar aluminum transducers with four different angles between their rectangular ports (0°, 45°, 90°, and 180°). The excellent experimental results validate the novel transducer with a measured converting efficiency higher than 98.2% in a 16.7% relative frequency bandwidth.

INDEX TERMS Waveguide mode transducer, TM_{01} circular waveguide mode, field pattern symmetry, mode-conversion purity, overmoded waveguide.

I. INTRODUCTION

Circular waveguides are usually excited by the fundamental TE_{11} mode in a large number of devices like filters, phase-shifters, ortho-mode transducer, etc [1]–[3]. In other kind of applications, the interest relies on working with field patterns that belong to higher-order modes. For example, the TE_{21} and TM_{01} modes are used in tracking systems for satellite communications [4]–[6]. Modes with azimuthal symmetry like TM_{01} and TE_{01} are essential in rotary joints to provide continuous rotating movement about the principal axis, preserving the electrical performance [7]–[10]. The circular waveguide TE_{01} mode has some special properties that make it suitable for low-loss transmission systems. Its electric field, without longitudinal and radial components, is not significantly affected by the outer wall conductivity, and its attenuation constant decreases with frequency. This behavior is also used in cylindrical cavities for obtaining TE_{01p} resonant modes with high quality factor for microwave filters, or for integration in other units with oscillators, gyrotrons, or high-energy systems, where frequency bands are progressively increasing and different modes need to be excited [12]–[17]. Furthermore, radial power combiners use extensively the TE_{01} circular waveguide mode [18]–[20].

In all the above applications, a transducer is compulsory to transfer the power carried by the fundamental mode in the input waveguide (typically rectangular, coaxial or circular) to the desired higher-order mode in the circular waveguide. In this work, the goal is to design a state of the art mode transducer from the rectangular waveguide TE_{10} mode to the circular waveguide TM_{01} mode, aiming to achieve a great performance at Ku-band with a topology suitable for accurate manufacturing.

Technical literature on this topic is very rich, from pioneer works in [7] to more recent works such as [21]–[23].

Besides, each frequency band has its own special features. A Ku-band transducer is designed in [22], using a door-knob probe and coaxial to circular waveguide transition in a 2.2% relative fractional bandwidth. On the other hand, [23] shows a X-band tunable transducer with a maximum tuning range of 500 MHz centered at 9.6 GHz, with 5.5% relative bandwidth. Therefore, there is a large margin for improvement as far as the bandwidth is concerned, and this has been one of the main challenges of this work. This issue is very important for modern systems operating in wider frequency bands, as the development of high-frequency amplification units based on solid state amplifiers. High-energy environments also benefit from devices with more bandwidth, avoiding the use of separate components for covering wider frequency bands. In this paper, a novel geometry is proposed and verified experimentally, obtaining a mode transducer with a measured converting efficiency of 98.2% in a 16.7% relative bandwidth.

This paper is organized as follows: section II describes the design of the transducer composed by the converting section and the feeding network with the T-type junctions, discussing the symmetries of both structures and the input excitation. In addition, the theoretical results of both elements and the complete transducer are presented. Experimental results are shown in section III validating the novel design. Finally, section IV summarizes the conclusions.
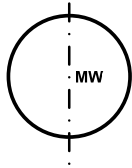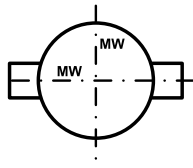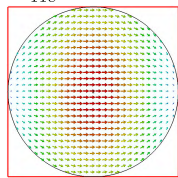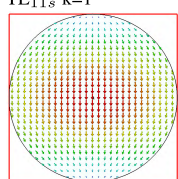
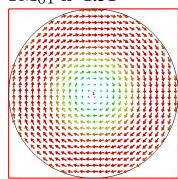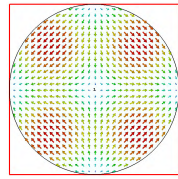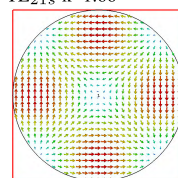## II. DESIGN OF THE TM_{01} MODE TRANSDUCER

The transducer proposed in this work is based on a T-type junction with sidewall coupling between a rectangular waveguide (standard *WR75* in *Ku-band*) and an external cylinder with the same height as the waveguide. The proper routing to the input excitation, which has to be with two fields with same in-phase polarization, will be the key for obtaining a great efficiency. Therefore, this transducer is composed by the elements shown in Fig. 1. The first element is the converting section, i.e., the structure combining the TE_{10} rectangular modes at the input into the TM_{01} circular mode at the output (part C in Fig. 1). The second element is the feeding network, routing the two arms of the converting section to the input (parts A and B in Fig. 1).

This topology has been selected for allowing an accurate manufacturing, as it will be seen later in section III, and, at the same time, can be devised in a modular and systematic way. This process will be used to achieve the following challenging electrical specifications: return loss level higher than 28 dB and attenuation level for the non-desired propagating mode TE_{11c} higher than 40 dB, from 11 to 13 (GHz), having a relative bandwidth of 16.7%.

A. BASIS OF THE TM_{01} MODE OPERATION: SYMMETRIES AND EXCITATION

Since the TM_{01} mode is not the fundamental mode of the circular waveguide, it is essential to analyze the symmetries of the electric and magnetic field patterns of its mode spectrum. This analysis must take into account the number of symmetry planes (1 or 2) of the involved building blocks,

TABLE 1. Circular waveguide modes associated to the cases of one symmetry (feeding network and mode transducer) or two symmetry planes (converting section), with Magnetic Wall (MW), their normalized cut-off frequencies and their magnetic field configuration.

Circular Waveguide Modes		
All modes	1 Magnetic Wall	2 Magnetic Walls
$k=\dfrac{f_c}{f_{c_{TE_{11}}}}$		
TE_{11c} k=1	TE_{11c} Excited	TE_{11c} Non-excited
TE_{11s} k=1	TE_{11s} Non-excited	TE_{11s} Non-excited
TM_{01} k=1.31	**TM_{01} Excited**	**TM_{01} Excited**
TE_{21c} k=1.66	TE_{21c} Non-Excited	TE_{21c} Non-Excited
TE_{21s} k=1.66	TE_{21s} Excited	TE_{21s} Excited

along with the field pattern of the excitation (the rectangular waveguide TE_{10} mode). Table 1 shows the modes associated to the cases of one symmetry plane (the feeding network and the final mode transducer) or two symmetry planes (the converting section). It also shows the normalized cut-off frequencies of the circular modes involved in each case, and their well-known magnetic field pattern for easier understanding. The electromagnetic field of the TM_{01} mode has Magnetic Wall (MW) symmetry (i.e., magnetic field is perpendicular to these planes as shown in Table 1) at the two principal planes
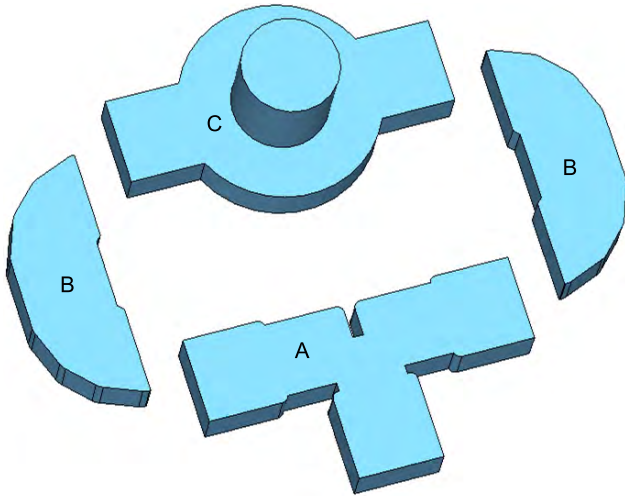
FIGURE 1. Different elements of the TM_{01} transducer: the converting section (part C) and the full H-plane feeding network composed by the T-junction (part A) and the two 180° bends (parts B).

of the part C in Fig. 1 acting as the converting section. However, the complete transducer (parts A+B+C) has only one physical symmetry plane. The different physical symmetries and the field symmetries that appear in the structure lead to the following cases:

1) When the converting section is analyzed as a separated building block, it has two physical symmetry planes and is excited with MW at both planes. Thus, when part C is considered alone, the first propagating mode in the circular waveguide is the TM_{01} (see second column in Table 1). The TE_{11} mode is not generated in this part C when it is excited with two in-phase signals with MW symmetry at its ports.

2) The feeding network composed of parts A and B is an H-plane structure (no variation along the height of the waveguide), and has only one physical symmetry plane. This means that when the feeding network is excited by the TE_{10} mode at the input of part A, the electromagnetic field at the output of the parts B, has not MW symmetry (although the field is not very far from having that MW symmetry). This MW symmetry can only be guaranteed when high-order modes (for instance the TE_{20} modes at the output of parts B) are fully suppressed. This could be done enlarging the waveguide connecting parts B and C (since these higher-order modes are evanescent for the operation band). However, a trade-off between compactness and performance is the preferred solution.

3) Consequently, the complete transducer integrated by parts A, B, and C has finally only one symmetry plane with MW boundary condition. In this case, the TE_{11s} mode is suppressed (see first column in Table 1), but the TE_{11c} can be excited (although very weakly if parts B and C have enough separation). Therefore, in the optimization of the complete transducer, the amplitude of

the propagating TE_{11c} is included in the cost function for keeping its level under the design requirement of 40 dB. The TE_{21s} mode is under cut-off in the bandwidth of interest and its attenuation level is controlled by the length of the output circular waveguide.

B. CONVERTING SECTION DESIGN BY A NOVEL T-TYPE JUNCTION WITH IN-PHASE EXCITATION

The converting section is based on a symmetrical right-angle T-type junction with output in circular waveguide with even excitation. Fig. 2 shows the proposed junction, which has a different field distribution with respect to a classical T-junction in E-plane configuration. This junction has two symmetry planes, which will be both working under MW boundary condition in order to avoid the generation of the TE_{11c} mode, as discussed before (see third column in Table 1). The lateral coupling between the two rectangular waveguides and the circular waveguide is as simpler as possible to simplify the manufacturing process. For this reason, avoiding any kind of iris or slot has been a priority in this design. However, it is mandatory to include some type of matching element to obtain the required return loss level in the specified bandwidth of operation.
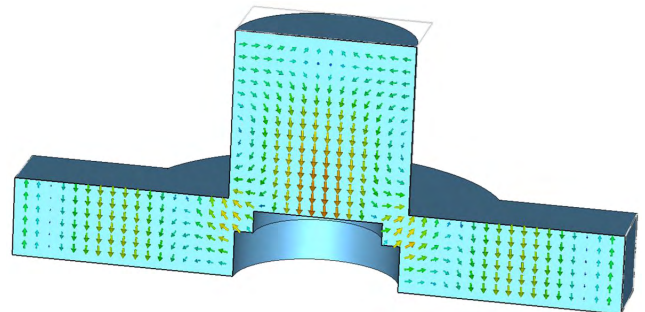

FIGURE 2. Longitudinal section of the T-type junction converting section showing the in-phase electric field in both rectangular ports.

Therefore, six parameters have been considered in the optimization process: the radius and height of two internal cylinders for matching, the radius of the external cylinder, and the radius of the output circular waveguide. Its final value is 10.77 mm, avoiding the propagation of the TE_{21c} mode. The height of the external cylinder is the same as the height of the WR75 standard waveguide, since in this way the manufacturing is highly simplified and the cost is reduced.

Fig. 3 shows the simulated return loss response of a quarter of the structure with MW boundaries conditions at the two symmetry planes. This reduces the computational effort in the simulations, which have been carried out by CST [24]. In addition, the TM_{01} is the only propagating mode in the operation band in the circular waveguide for this problem. In the inset, it can be observed the direct connection between the standard *WR75* and the external cylinder without irises, and the two internal cylinders for matching. Finally, Fig. 2 shows the longitudinal section of the converting section based
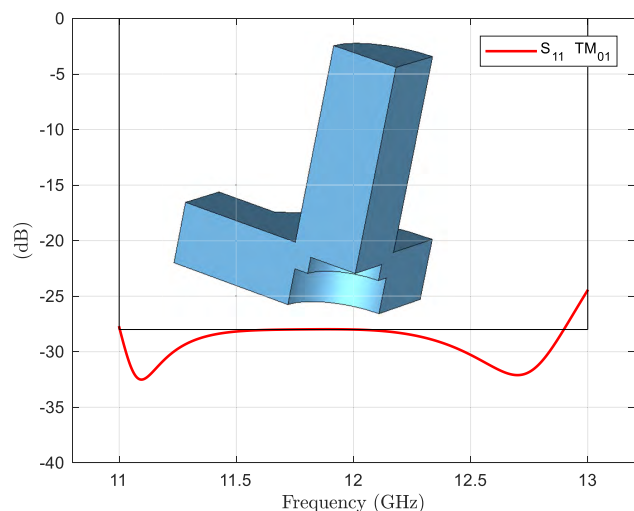
FIGURE 3. Simulated return loss of the coverting-section for the TM$_{01}$ mode at the circular waveguide. In the inset, one quarter of the structure with MW boundary conditions applied at the two symmetry planes of part C in Fig.1.

FIGURE 4. Simulated return loss for the the TE$_{10r}$ at the input port of the T-junction in H-plane configuration considering rounded corners. In the inset, the structure shows the septum and waveguides steps to improve the bandwidth response.

on the proposed T-type junction, showing the in-phase electric field at both rectangular ports.

C. FEEDING NETWORK DESIGN WITH AN H-PLANE T-JUNCTION

Once the converting section has been designed, its two excitation ports must be routed to the input by means of the feeding network, preserving the symmetry plane (see second column in Table 1). This network is shown in Fig. 1 and is composed by an H-plane T-junction (part A) and 180° waveguide bends (parts B), all in H-plane configuration. All these building blocks have the height of the standard *WR75* waveguide, which is used at the input. The T-junction includes a septum and an small step for improving the matching in the required bandwidth. Parts A and B have been designed separately and then connected together achieving a return loss level higher than 30 dB. In the optimization process of both parts A and B, the rounded corners due to the radius of the milling tool used in the manufacturing have been taken into account in the optimization process. Fig. 4 shows the simulated return loss of the input of the H-plane T-junction (part A) after the optimization considering the rounded corners. Fig. 5 shows the simulated return loss of the 180° waveguide bend (part B).

D. FINAL DESIGN OF THE COMPLETE MODE TRANSDUCER

According to the described step-by-step procedure, the two elements of the transducer, i.e., the converting section and the feeding network, designed separately, are now connected. In this last stage, a final optimization is carried out to fulfill the specifications of return loss level and high-purity conversion. It is worth to note that one of the symmetry planes disappears now, and. as a result, the TE$_{11c}$ circular mode is not suppressed by symmetry considerations. Nevertheless, its
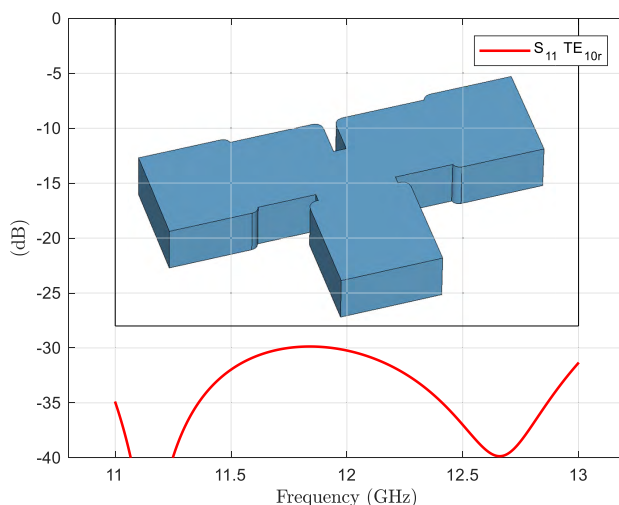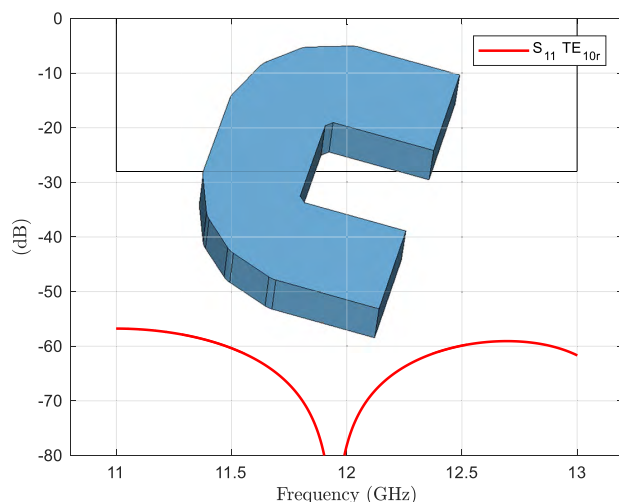

FIGURE 5. Simulated return loss of the 180° H-plane bend. In the inset, the optimized structure with rounded corners.

level can be controlled by the length connecting the 180° waveguide bend to the converting section since its attenuation level must be larger than 40 dB.

Fig. 6 shows the simulated return loss of the complete transducer with a value higher than 28 dB for the TE$_{10r}$ rectangular mode (the *r* in the sub-index is for identifying that belongs to the rectangular waveguide) and for the TM$_{01}$ circular mode. Besides, this figure shows the attenuation of the TE$_{11c}$ circular mode, higher than 40 dB, when exciting in the corresponding port by the TE$_{10r}$ rectangular mode and by the TM$_{01}$ circular mode. The responses are computed in a 2 GHz bandwidth centered at 12 GHz (16.7% relative bandwidth). The inset shows the electric field conversion between the input TE$_{10}$ mode in the rectangular waveguide and the output TM$_{01}$ mode in the circular waveguide.
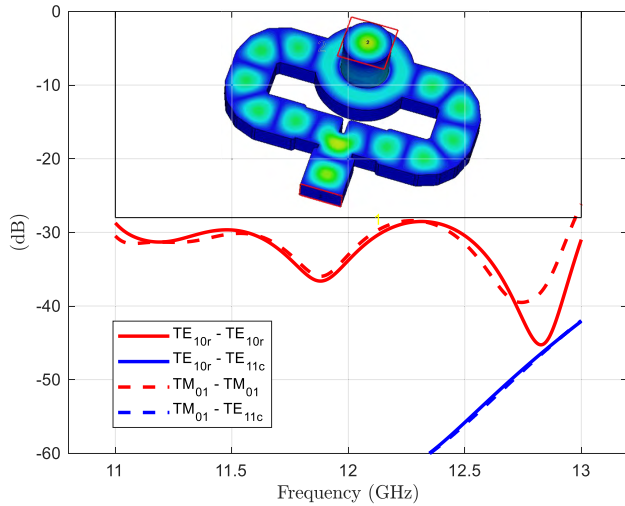
FIGURE 6. Simulated response of the complete transducer: return loss for the TE_{10r} rectangular mode (solid red line) and TM_{01} circular mode (dashed red line), attenuation of the TE_{11c} circular mode (transmission from the TE_{10r} at the rectangular port to the TE_{11c} at the circular port, solid blue line), and attenuation of the TE_{11c} circular mode (transmission from the TM_{01} at the circular port to the TE_{11c} at the circular port, dashed blue line). In the inset, the electric field configuration is shown.

FIGURE 7. Back-to-back configuration of two similar transducers and four different angles between input and output ports (0°, 45°, 90° and 180°) to verify the purity of the TM_{01} by means of the insertion loss and return loss measurements.

Considering the use of the transducer in high-energy applications, such as particle accelerators, plasma heating, etc., its power handling has been calculated at the lowest frequency of operation (11 GHz). Assuming a break-down field of 30 kV/cm, corresponding to the device filled with air, a 320 kW value has been computed for the most critical dimension in the converting section. However, the power handling level can be increased dramatically filling the device with an insulator gas like SF_6.

III. EXPERIMENTAL RESULTS

The topology for the transducer has been selected taking into account a suitable mechanical segmentation for the full structure in a main body and a cover. In order to verify the theoretical results, two equal transducers have been manufactured in aluminum using Computer Numerical Control (CNC) machining for the two parts of each transducer, i.e., the body and the cover. The insertion loss and the return loss have been measured in a back-to-back configuration. As in other works related to transducers [19], [23] this is the usual way to test this type of experimental prototypes involving higher-order modes whose direct characterization is not direct. In addition, as Fig. 7 shows, four different angles between the input and output ports (0°, 45°, 90° and 180°) have been tested in order to verify the purity of the generation of the TM_{01} mode. The measured results will show that the angle of connection does not affect the performance, as it would be expected due to the azimuthal symmetry of the field pattern.

Fig. 8 shows the comparison between the simulated insertion loss with 0° angle (see the inset in this figure) and the four measurements corresponding to the four different angles, considering an effective conductivity for the
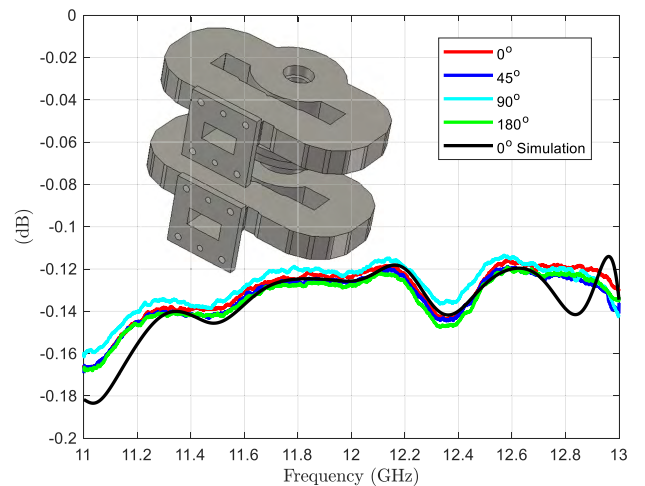

FIGURE 8. Comparison of the insertion loss between the full-wave simulation of the transducer in a back-to-back configuration and the four measurements with 0°, 45°, 90° and 180° angles between the input and output waveguides, considering an effective conductivity for the aluminum $\sigma_{eff} = 12.2\ MS/m$. In the inset, a 3D CAD view with the case of 0° angle is shown for reference.

aluminum $\sigma_{eff} = 12.2$ MS/m. This value takes into account the roughness of the walls and the manufacturing process. As it can be observed, the agrement is very good and the four measurements superimpose onto each other. The highest value of the insertion loss for one transducer is 0.08 dB. If the converting efficiency of a specific mode is defined as its transmission coefficient [25], i.e., using $|s_{21}|^2$, the worst measured value is 98.2% in the 16.7% relative bandwidth of the design, an excellent result.

Fig. 9 shows the comparison of the simulated return loss with 0° angle rotation (see the inset in the figure) and the
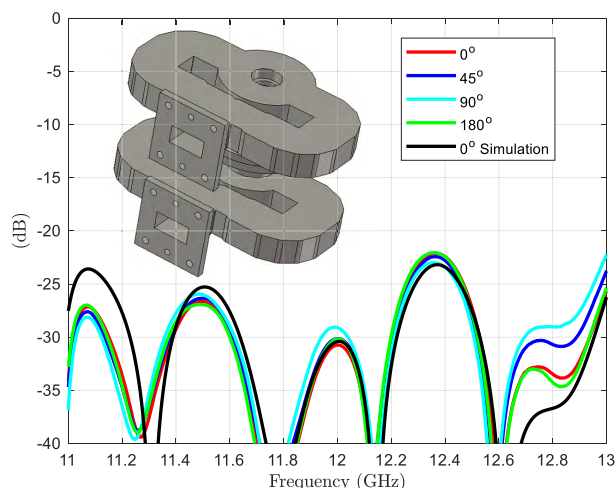
FIGURE 9. Comparison of the return loss between the simulation of the transducer in a back-to-back configuration and the four measurements with 0°, 45°, 90° and 180° angles between the input and output waveguides, considering an effective conductivity for the aluminum $\sigma_{eff} = 12.2\ MS/m$. In the inset, a 3D CAD view with the case 0° angle is shown as reference.
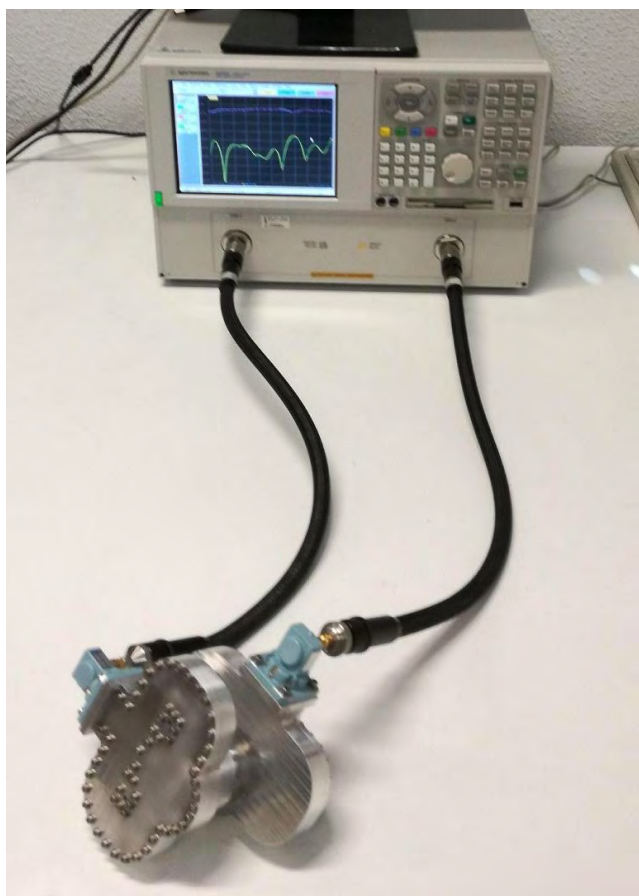

FIGURE 10. Manufactured prototype in the measurement bench with 90° angle between input output ports in the back-to-back configuration.

four measurements corresponding to the four angles, considering the same effective conductivity for the aluminum as previously. It is worth to highlight the overlapping of

the four measurements. This reveals again the purity of the conversion and the negligible relevance of the propagating mode TE_{11c} (not suppressed by the symmetry of the structure for the cases of 0°, 45°, 90° and 180°) and TE_{11s} (not suppressed by the symmetry of the structure for the cases of 45° and 90°). Fig. 10 shows the transducer during the experimental characterization of the back-to-back configuration with 90° angle between ports, connected to the Vector Network Analyzer (VNA).

IV. CONCLUSION

This papers presents a novel TM_{01} mode transducer with, to the authors' knowledge, state of the art performance in Ku-band: return loss loss level higher than 28 dB (23 dB measured in back-to-back configuration) and attenuation of the non-desired propagating mode TE_{11c} higher than 40 dB, in a 16.7% relative bandwidth, This result is obtained with a novel waveguide arrangement based on two in-phase T-type junctions. A systematic design method has been presented for the two elements of the transducer (the converting section and the feeding network), based on a deep study of symmetries and boundary conditions for controlling the different modes, which is also used to reduce the computational effort.

In addition, the physical structure has been simplified to ease the manufacturing, since the transducer can be segmented in a simple configuration of a main body and a cover. In view that milling can be used to fabricate the two parts, the cost is dramatically reduced. Finally, in order to verify the theoretical results, a back-to-back measurement has been carried out with four different angles between the input and output ports. The excellent experimental results, with a measured converting efficiency of 98.2% in a 16.7% relative bandwidth, validate the new proposed transducer.

REFERENCES

[1] G. Matthei, E. M. T. Jones, and L. Young, *Microwave Filters, Impedance-Matching Networks, and Coupling Structures*. Norwood, MA, USA: Artech House, 1980.

[2] C. G. Montgomery, R. H. Dicke, and E. M. Purcell, *Principles of Microwave Circuits*. London, U.K: IEE Electromagnetic Waves Series, 1987.

[3] J. Uher, J. Bornemann, and U. Rosenberg, *Waveguide Components for Antenna Feed Systems: Theory and CAD*. Boston, MA, USA: Artech House, ch. 3, 1993.

[4] G. J. Hawkins, D. J. Edwards, and J. P. McGeehan, "Tracking systems for satellite communications," *IEE Proc. F Radar Signal Process.*, vol. 135, no. 5, pp. 393–407, Oct. 1988.

[5] E. H. Lenzing and H. F. Lenzing, "Characteristics of the TE_{21}^0 mode in circular apertures as used for satellite tracking," *IEEE Trans. Aerosp. Electron. Syst.*, vol. 37, no. 3, pp. 1113–1117, Jul. 2001.

[6] S. M. M. Azizi and S. H. M. Armaki, "A compact TE_{21} mode coupler for tracking purposes," *IEEE Microw. Wireless Compon. Lett.*, vol. 28, no. 6, pp. 470–472, Jun. 2018.

[7] G. L. Ragan, *Microwave Transmission Circuits* (MIT Radiation Laboratory Series), vol. 9. New York, NY, USA: McGraw-Hill, 1948.

[8] A. F. Harvey, *Microwave Engineering*, New York, NY, USA: Academic, 1963.

[9] J. Helszajn, *Passive and Active Microwave Circuits*. Hoboken, NJ, USA: Wiley, 1978.

[10] A. Yevdokymov, V. Kryzhanovskiy, V. Pazynin, and K. Sirenko, "Ka-band waveguide rotary joint," *IET Microw., Antennas Propag.*, vol. 7, no. 5, pp. 365–369, Apr. 2013.

[11] G. Southworth, *Principles and Applications of Waveguide Transmission* (The Bell Telephone Laboratories Series). New York, NY, USA: Van Nostrand, 1956.

[12] K. R. Chu, "The electron cyclotron maser," *Rev. Mod. Phys.*, vol. 76, no. 2, p. 489, May 2004.

[13] M. Blank, B. G. Danly, and B. Levush, "Experimental demonstration of a W-band (94 GHz) gyrotron amplifier," *IEEE Trans. Plasma Sci.*, vol. 27, no. 2, pp. 405–411, Apr. 1999.

[14] K. C. Leou, D. B. McDermott, A. J. Balkcum, and N. C. Luhmann, "Stable high-power TE_{01} gyro-TWT amplifiers," *IEEE Trans. Plasma Sci.*, vol. 22, no. 5, pp. 585–592, Oct. 1994.

[15] M. Garven *et al.*, "A gyrotron-traveling-wave tube amplifier experiment with a ceramic loaded interaction region," *IEEE Trans. Plasma Sci.*, vol. 30, no. 3, pp. 885–893, Jun. 2002.

[16] W. He, C. R. Donaldson, L. Zhang, K. Ronald, A. D. R. Phelps, and A. W. Cross, "Broadband amplification of low-terahertz signals using axis-encircling electrons in a helically corrugated interaction region," *Phys. Rev. Lett.*, vol. 119, no. 18, p. 184801, 2017.

[17] L. Zhang, C. R. Donaldson, J. Garner, A. W. Cross, and W. He, "Input coupling systems for millimetre-wave gyrotron travelling wave amplifiers," *IET Microw., Antennas Propag.*, vol. 12, no. 11, pp. 1748–1751, Dec. 2018, doi: 10.1049/iet-map.2018.0040.

[18] M. H. Chen, "A 19-way isolated power divider via the TE_{01} circular waveguide mode transition," in *IEEE MTT-S Int. Microw. Symp. Dig.*, Jun. 1986, pp. 511–513.

[19] J. R. Montejo-Garai, I. Saracho-Pantoja, J. A. Ruiz-Cruz, and J. M. Rebollar, "High-performance 16-way Ku-band radial power combiner based on the TE_{01}-circular waveguide mode editors'-pick," *Rev. Sci. Instrum.*, vol. 89, no. 3, p. 034703, 2018.

[20] J. R. Montejo-Garai, J. A. Ruiz-Cruz, and J. M. Rebollar, "5-way radial power combiner at w-band by stacked waveguide micromachining," *Nucl. Instrum. Methods Phys. Res. Sect. A, Accel., Spectrometers, Detect. Associated Equip.*, vol. 905, pp. 91–95, Oct. 2018.

[21] X.-M. Li, J.-Q. Zhang, X.-Q. Li, and Q.-X. Liu, "A high-power orthogonal over-mode circular waveguide TE_{11}-TM_{01} mode converter," *IEEE Microw. Wireless Compon. Lett.*, vol. 27, no. 12, pp. 1095–1097, Dec. 2017.

[22] S. B. Chakrabarty, V. K. Singh, and S. B. Sharma, "TM_{01} mode transducer using circular and rectangular waveguides," *Int. J. RF Microw. Comput.-Aided Eng.*, vol. 20, no. 3, pp. 259–263, May 2010.

[23] A. Cui *et al.*, "High-efficiency, broadband converter from a rectangular waveguide TE_{01} mode to a circular waveguide TM_{01} mode for overmoded device measurement," *IEEE Access*, vol. 6, pp. 14996–15003, 2018.

[24] Computer Simulation Technology. Accessed: Dec. 2018. [Online]. Available: https://www.cst.com/

[25] C.-F. Yu and T.-H. Chang, "High-performance circular TE_{01}-mode converter," *IEEE Trans. Microw. Theory Tech.*, vol. 53, no. 12, pp. 3794–3798, Dec. 2005.

JOSÉ R. MONTEJO-GARAI was born in Vitoria-Gasteiz, Spain, in 1965. He received the Ingeniero de Telecomunicación and Ph.D. degrees from the Universidad Politécnica de Madrid, Madrid, Spain, in 1990 and 1994, respectively. Since 1989, he has been with the Grupo de Electromagnetismo Aplicado y Microondas, Universidad Politécnica de Madrid, as an Assistant Professor, until 1996, and as an Associate Professor until 2017, where he is currently a Full Professor. His current research interests include the analysis and characterization of wave-guide structures, advanced synthesis theory, and computer aided design for microwave and millimeter-wave passive devices: filters, multiplexers, orthomode transducers, and beam forming networks. He has designed a plenty of passive microwave devices for communication satellites.

JORGE A. RUIZ-CRUZ (SM'11) received the Ingeniero de Telecomunicación and Ph.D. degrees from the Universidad Politécnica de Madrid, Madrid, Spain, in 1999 and 2005, respectively. Since 2006, he has been with the Universidad Autónoma de Madrid, Madrid, where he became an Associate Professor, in 2009. His current research interests include the computer-aided design of microwave passive devices and circuits (filters, multiplexers, and orthomodes).

JESÚS M. REBOLLAR (M'15) was born in Beasain, Spain, in 1953. He received the Ingeniero de Telecomunicación and Ph.D. degrees from the Universidad Politécnica de Madrid, Madrid, Spain, in 1975 and 1980, respectively. Since 1976, he has been with the Grupo de Electromagnetismo Aplicado y Microondas, Universidad Politécnica de Madrid, as an Assistant Professor, until 1982, and as an Associate Professor, until 1988, where he was appointed as a Professor of teoría electromagnética. His current research interests include electromagnetic wave propagation in waveguide structures, interactions of electromagnetic fields with biological tissues, and particularly computer aided design for microwave and millimeter-wave passive devices: filters, multiplexers, polarizers, orthomode transducers, and beam forming networks. He has designed many of the above components for communication systems on-board satellites.

• • •